IL NUOVO CIMENTO Vol. 36 C, N. 6 Novembre-Dicembre 2013
DOI 10.1393/ncc/i2014-11629-2

Colloquia: LaThuile13

# $b$-baryon mass measurements at LHCb

R. Märki(*)
*Ecole Polytechnique Fédérale de Lausanne (EPFL) - Lausanne, Switzerland*

ricevuto il 20 Giugno 2013; approvato l'1 Luglio 2013

**Summary.** — Hadrons are systems bound by the strong interaction, which is described at the fundamental level by Quantum Chromodynamics (QCD). Several models and techniques, such as constituent-quark models or lattice-QCD calculations, attempt to reproduce the spectrum of b-hadron masses. On the experimental side, while the masses of all expected ground-state mesons are now well measured, baryon data are still sparse. The LHCb experiment at CERN's Large Hadron Collider is dedicated to bottom physics and $CP$ violation. The first $1.0\,\text{fb}^{-1}$ of $pp$ collisions collected during the 2011 run allows the exploration of the $b$-baryon sector with unprecedented precision. We present the most precise measurements of the $\Lambda_b^0$, $\Xi_b^-$ and $\Omega_b^-$ baryon masses to date.

PACS 14.20.Mr – Bottom baryons ($|B| > 0$).

## 1. – Introduction

Several properties of bottom baryons such as masses, lifetimes and production rates, are predicted using Quantum Chromodynamics (QCD) calculations. To date, the most accurate theoretical mass predictions in terms of uncertainties are obtained with constituent-quark models [1]. Other attempts using different techniques such as the QCD sum rule approach to the HQET framework or lattice-QCD calculations provide compatible results [2-8]. Experimentally, only single-$b$ baryons have been observed so far and few precise measurements of their masses, lifetimes and productions rates exist.

The first $b$ baryon to be observed and have its mass measured was the $\Lambda_b^0$ [9]. Between 2007 and 2009 the D0 and CDF experiments observed the $\Xi_b^-$ and $\Omega_b^-$ baryons and measured their masses [10-12]. They agree on the $\Xi_b^-$ mass but disagree at the 6 $\sigma$ level about the $\Omega_b^-$ one. Using $1\,\text{fb}^{-1}$ of $pp$ collisions at a centre-of-mass energy of $\sqrt{s} = 7\,\text{TeV}$ recorded with the LHCb detector during the year 2011, we are able to extend

(*) E-mail: raphael.marki@epfl.ch

 

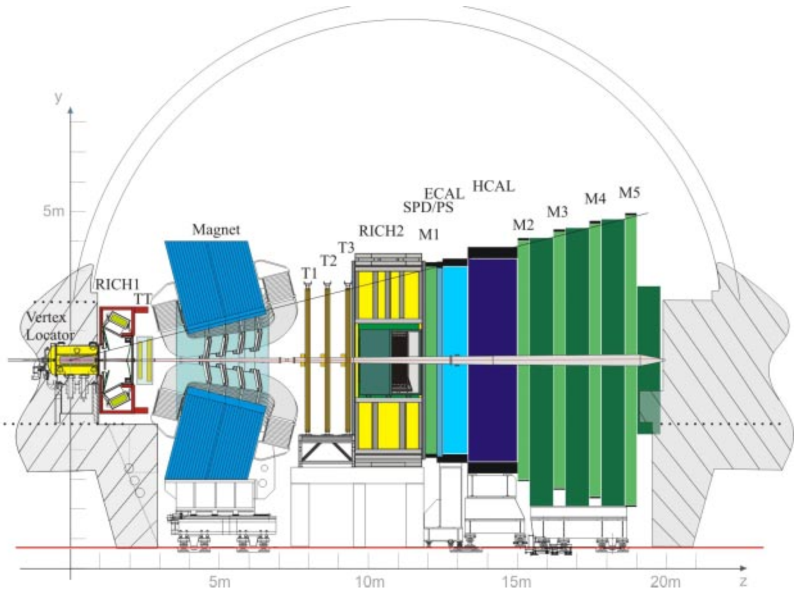


Fig. 1. – Schematic view of the LHCb detector.

the knowledge about weakly decaying bottom baryons. High-precision measurements of the $\Lambda_b^0$, $\Xi_b^-$ and $\Omega_b^-$ masses have been performed and are reported hereafter.

The LHCb detector [13], shown in fig. 1, is a single-arm forward spectrometer covering the pseudorapidity range $2 < \eta < 5$, designed for the study of particles containing $c$ or $b$ quarks. The detector includes a high precision tracking system consisting of a silicon-strip vertex detector surrounding the $pp$ interaction region, a large-area silicon-strip detector located upstream of a dipole magnet with a bending power of about 4 Tm, and three stations of silicon-strip detectors and straw drift tubes placed downstream. The combined tracking system has a momentum resolution $\Delta p/p$ that varies from 0.4% at 5 GeV/$c$ to 0.6% at 100 GeV/$c$, and an impact parameter resolution of 20 $\mu$m for tracks with high transverse momentum. Charged hadrons are identified using two ring-imaging Cherenkov detectors. Photon, electron and hadron candidates are identified by a calorimeter system consisting of scintillating-pad and preshower detectors, an electromagnetic calorimeter and a hadronic calorimeter. Muons are identified by a system composed of alternating layers of iron and multiwire proportional chambers. The trigger [14] consists of a hardware stage, based on information from the calorimeter and muon systems, followed by a software stage which applies a full event reconstruction.

## 2. – Momentum scale calibration

In order to accurately measure invariant masses, the momentum of all daughter particles must be known with high precision. At LHCb, the momenta of charged particles are measured using the tracking devices on both sides of the magnetic field. The precision of momentum measurements is limited by the imperfect alignment and the finite knowledge of the magnetic field. To extend the precision, a momentum scale calibration is applied which compensates for these two effects.

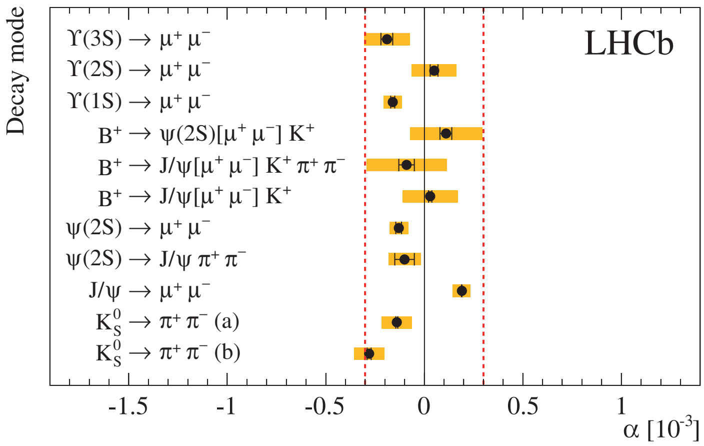


Fig. 2. – Average momentum scale bias $\alpha$ determined from the reconstructed mass of various decay modes after the momentum calibration procedure. The $K^0_S$ decays are divided into two categories according to whether both daughter tracks (a) have hits or (b) do not have hits in the vertex detector. The black error bars represent the statistical uncertainty whilst the (yellow) filled areas also include contributions to the systematic uncertainty from the fitting procedure, the effect of QED radiative corrections, and the uncertainty on the mass of the decaying meson [15]. The (red) dashed lines show the assigned uncertainty of $\pm 0.3 \times 10^{-3}$ on the momentum scale.

In a first step, the data taking period is divided into 12 sub-ranges. For each sub-range, a correction factor for the momentum is applied based on the measured $J/\psi \to \mu^+\mu^-$ mass as compared to the known value.

In the second step one estimates the absolute momentum scale which is based on the high-statistics $B^+ \to J/\psi K^+$ decay. There, the $J/\psi$ mass is constrained to its known value which leaves the $K^+$ momentum as the only contributing parameter. Since the calibration depends only on this track, we split the sample into bins of track slope ($T_x = p_x/p_z$ and $T_y = p_y/p_z$) of the $K^+$ track. Therefore the momentum calibration is performed separately in such bins.

Finally, the residual bias is evaluated by comparing the masses of other reconstructed resonances to their known value, as shown in fig. 2. The residual bias is called $\alpha$ and is calculated so that multiplying the momentum of every final state track by $(1-\alpha)$, the reconstructed invariant mass is shifted to the PDG mass. We assigned an error on the momentum scale of $\alpha_{\max} = \pm 0.3 \times 10^3$.

## 3. – Mass measurements

All candidates are selected with cuts. The $\Lambda^0_b$ selection is based on the selection with 2010 data [16] whereas the other two selections were optimized using relative yield estimates from CDF and D0. In the end, the $\Xi^-_b$ and $\Omega^-_b$ selections are almost identical. We take particular advantage of the decay topology by cutting on the flight distance. In all three cases we use tracks with and without vertex detector information.

For all three channels, the mass was obtained by performing an extended unbinned maximum-likelihood fit, shown in fig. 3. The signal is described with a single (double)

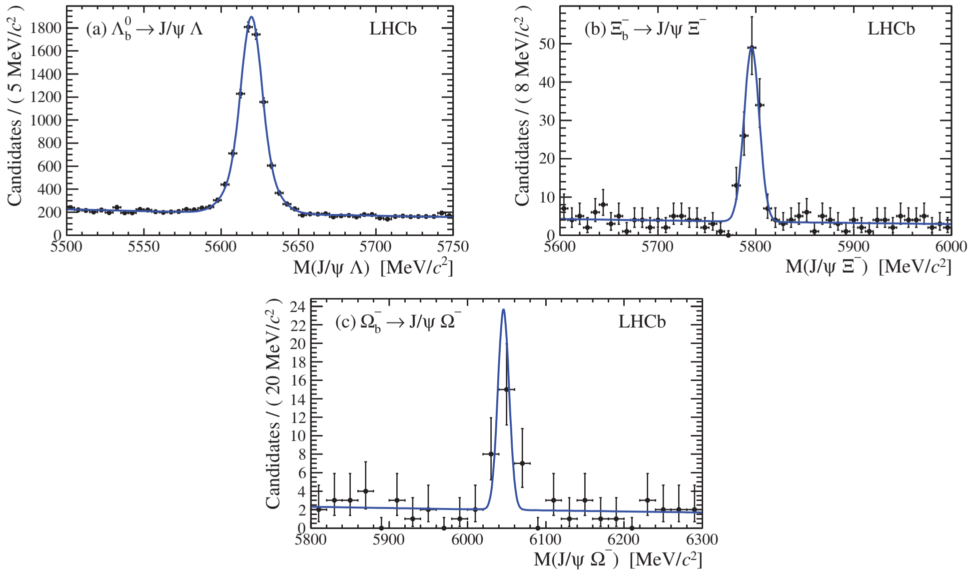


Fig. 3. – Invariant mass distribution for (a) $\Lambda_b^0 \to J/\psi\Lambda$, (b) $\Xi_b^- \to J/\psi\Xi^-$ and (c) $\Omega_b^- \to J/\psi\Omega^-$ candidates. The results of the unbinned maximum-likelihood fits are shown with solid lines.

Gaussian function for the $\Xi_b^-$ and $\Omega_b^-$ ($\Lambda_b^0$) channels. In the case of the $\Omega_b^-$ baryon, the width of the Gaussian function is constrained to the $\Xi_b^-$ width multiplied by the appropriate width ratio from simulation. The background is modelled in all three cases with an exponential function. The yields, widths and masses with their respective statistical uncertainties are reported in table I.

The statistical significance of the $\Omega_b^-$ signal has been studied using simulated pseudo-experiments to take into account the so-called look-elsewhere effect [17]. The significance was found to be greater than 6 standard deviations.

The fits and the candidate reconstruction are both repeated varying in turn all parameters within their uncertainty. The difference with respect to nominal fit is then taken as the systematic uncertainty on the mass measurement. The considered sources of uncertainty are the momentum scale, energy loss ($\mathrm{d}E/\mathrm{d}x$) corrections and the fit parameters for signal and background. A calculation of the effect of the uncertainty on the constrained hyperon mass is also performed and included as a source of systematic uncertainty. All systematic uncertainties are summarised in table II.

TABLE I. – *Results of the fits to the invariant mass distributions. The quoted uncertainties are statistical. The $\Lambda_b^0$ signal is described by a double Gaussian function with widths $\sigma_1$ and $\sigma_2$; the fraction of the yield described by the first component is* $0.58 \pm 0.11$.

| | Signal yield | Mass [MeV/$c^2$] | Width(s) [MeV/$c^2$] |
|---|---|---|---|
| $\Lambda_b^0$ | $6870 \pm 110$ | $5619.53 \pm 0.13$ | $\sigma_1 = 6.4 \pm 0.5$<br>$\sigma_2 = 12.5 \pm 1.3$ |
| $\Xi_b^-$ | $111 \pm 12$ | $5795.8 \pm 0.9$ | $7.8 \pm 0.7$ |
| $\Omega_b^-$ | $19 \pm 5$ | $6046.0 \pm 2.2$ | 7.2 (fixed) |

TABLE II. – *Systematic uncertainties (in* MeV/$c^2$*) on the mass measurements and their differences. The total systematic uncertainty is obtained from adding all uncertainties in quadrature.*

| Source | $\Lambda_b^0$ | $\Xi_b^-$ | $\Omega_b^-$ | $\Xi_b^-$–$\Lambda_b^0$ | $\Omega_b^-$–$\Lambda_b^0$ |
|---|---|---|---|---|---|
| Momentum scale | 0.43 | 0.43 | 0.31 | 0.01 | 0.12 |
| d$E$/d$x$ correction | 0.09 | 0.09 | 0.09 | 0.01 | 0.01 |
| Hyperon mass | 0.01 | 0.07 | 0.25 | 0.07 | 0.25 |
| Signal model | 0.07 | 0.01 | 0.24 | 0.07 | 0.25 |
| Background model | 0.01 | 0.01 | 0.02 | 0.01 | 0.02 |
| Total | 0.45 | 0.45 | 0.47 | 0.10 | 0.37 |

The largest systematic uncertainty comes from the momentum calibration. In mass differences, it strongly cancels which lets the hyperon mass constraint and signal model become the most significant contribution.

## 4. – Summary

LHCb provides the most precise $\Lambda_b^0$, $\Xi_b^-$ and $\Omega_b^-$ mass measurements to date:

$$\begin{aligned} M(\Lambda_b^0) &= 5619.53 \pm 0.13\ (\text{stat}) \pm 0.45\ (\text{syst})\,\text{MeV}/c^2,\\ M(\Xi_b^-) &= 5795.8 \pm 0.9\ (\text{stat}) \pm 0.4\ (\text{syst})\,\text{MeV}/c^2,\\ M(\Omega_b^-) &= 6046.0 \pm 2.2\ (\text{stat}) \pm 0.5\ (\text{syst})\,\text{MeV}/c^2. \end{aligned}$$

The dominant systematic uncertainty, due to the knowledge of the momentum scale, partially cancels in mass differences. We obtain

$$\begin{aligned} M(\Xi_b^-) - M(\Lambda_b^0) &= 176.2 \pm 0.9\ (\text{stat}) \pm 0.1\ (\text{syst})\,\text{MeV}/c^2,\\ M(\Omega_b^-) - M(\Lambda_b^0) &= 426.4 \pm 2.2\ (\text{stat}) \pm 0.4\ (\text{syst})\,\text{MeV}/c^2. \end{aligned}$$

The $\Lambda_b^0$ and $\Xi_b^-$ results are in agreement with previous measurements. The $\Omega_b^-$ result is in agreement with the CDF measurement [12], but in disagreement with the D0 measurement [11].

Combining the measurement of the $\Lambda_b^0$ mass with the previous LHCb result performed using 35 pb$^{-1}$ of data recorded during the year 2010 [16] yields

$$M(\Lambda_b^0) = 5619.44 \pm 0.13 \pm 0.38\,\text{MeV}/c^2.$$

All measurements are compared in fig. 4 with the most precise measurements from ATLAS, CDF and D0, and with the current world averages [15].

New $b$-baryon measurements including 2011 and 2012 data (1 fb$^{-1}$ + 2 fb$^{-1}$) are soon to come. The lifetimes of $\Lambda_b^0$, $\Xi_b^-$ and $\Omega_b^-$ are among the studies with high priority. In addition, there are excellent prospects for further spectroscopy at LHCb in the years to come. Additional 5 fb$^{-1}$ of data at least are expected by 2017 with a $b$-hadron production cross section twice as large.

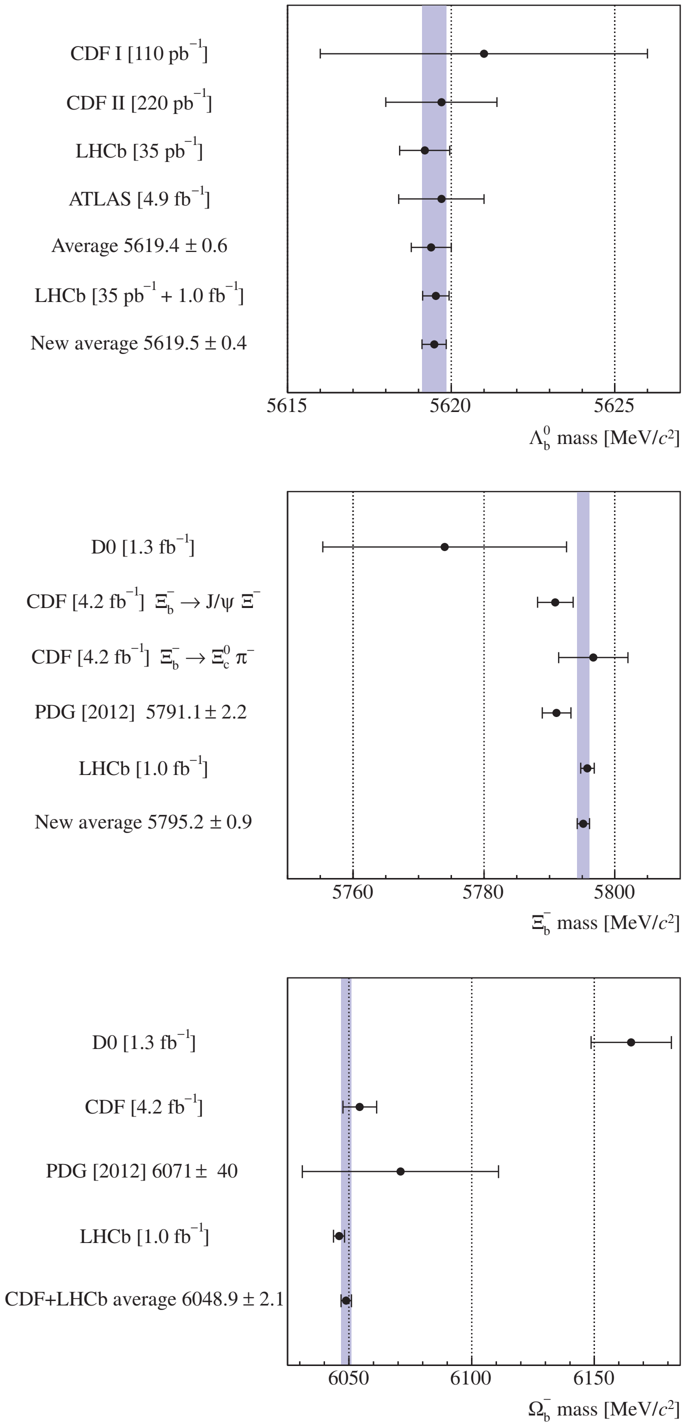


Fig. 4. – Comparison between LHCb measurements and previous most precise measurements of ATLAS, CDF and D0.

## REFERENCES

[1] Karliner M., Keren-Zur B., Lipkin H. J. and Rosner J. L., *Ann. Phys. (N.Y.)*, **342** (2009) 2 arXiv:0804.1575.
[2] Day J. P., Plessas W. and Choi K.-S., arXiv:1205.6918 (2012).
[3] Liu X., Chen H.-X., Liu Y.-R., Hosaka A. and Zhu S.-L., *Phys. Rev. D*, **77** (2008) 014031 arXiv:0710.0123.
[4] Zhang J.-R. and Huang M.-Q., *Phys. Rev. D*, **78** (2008) 094015 arXiv:0811.3266.
[5] Jenkins E. E., *Phys. Rev. D*, **77** (2008) 034012 arXiv:0712.0406.
[6] Roncaglia R., Lichtenberg D. B. and Predazzi E., *Phys. Rev. D*, **52** (1995) 1722 arXiv:hep-ph/9502251.
[7] Lewis R. and Woloshyn R. M., *Phys. Rev. D*, **79** (2009) 014502 arXiv:0806.4783.
[8] Ebert D., Faustov R. N. and Galkin V. O., *Phys. Rev. D*, **72** (2005) 034026 arXiv:hep-ph/0504112.
[9] Albajar C. *et al.* (UA1 Collaboration), *Phys. Lett. B*, **273** (1991) 540.
[10] Abazov V. M. *et al.* (D0 Collaboration), *Phys. Rev. Lett.*, **99** (2007) 052001 arXiv:0706.1690.
[11] Abazov V. M. *et al.* (D0 Collaboration), *Phys. Rev. Lett.*, **101** (2008) 232002 arXiv:0808.4142.
[12] Aaltonen T. *et al.* (CDF Collaboration), *Phys. Rev. D*, **80** (2009) 072003 arXiv:0905.3123.
[13] Alves Jr. A. A. *et al.* (LHCb Collaboration), *JINST*, **3** (2008) S08005.
[14] Aaij R. *et al.*, arXiv:1211.3055 (2012).
[15] Beringer J. *et al.* (Particle Data Group), *Phys. Rev. D*, **86** (2012) 010001.
[16] Aaij R. *et al.* (LHCb Collaboration), *Phys. Lett. B*, **708** (2012) 241 arXiv:1112.4896.
[17] Gross E. and Vitells O., *Eur. Phys. J. C*, **70** (2010) 525 arXiv:1005.1891.